Eigenerosion for static and dynamic brittle fracture

Flavio Stochino[a], Aurel Qinami[b], Michael Kaliske [b,*]

[a]*Department of Civil, Environmental Engineering, University of Cagliari, 09123 Cagliari, Italy*
[b]*Institute for Structural Analysis, Technische Universität Dresden, 01062 Dresden, Germany*

Abstract

In contrast to many numerical methods, the eigenerosion approach yields a convenient description of fracture handled in the postprocessing part of a Finite Element Analysis (FEA). Its fully energetic formulation avoids the introduction of extra degrees of freedom to model fracture propagation. Following previous works on eigenerosion, in this publication, a modified formulation of eigenfracture it is introduced, where it is distinguished between compression and tension loaded state. This formulation has the advantage that it relates the crack propagation process only to tensile loading. The procedure is implemented using a spectral decomposition of the strain field. The application of the method to brittle fracture makes it suitable for materials like concrete. The accuracy of the method is assessed for linear elasticity in statics and dynamics for two- and three-dimensional problems.

Keywords: fracture mechanics, concrete, eigenfracture, eigenerosion

1. Introduction

Since the catastrophic failures of tankers and cargo ships during World War II [1], the awareness of the importance of fracture mechanics has been strongly increased. Actually, the first study on fracture is associated with Leonardo da Vinci who noted that a shorter wire was more resistant to tensile yielding than a longer one, see [2]. But only centuries later, thanks to Griffith's work [3], the first theoretical model for fracture propagation in brittle materials was obtained. It is based on a simple energy balance

*michael.kaliske@tu-dresden.de

criterion between the energy released to the system and the one dissipated by the fracture process. Since then, the generalized Griffith theory of brittle fracture has been studied and applied in order to model fracture propagation as a *free-discontinuity problem*. A very interesting approach, which opened a lot of potential for numerical implementations of fracture, was presented by Francfort and Marigo [4] and then applied and improved by Dal Maso and Toader [5, 6, 7].

In particular, a promising approximation scheme for variational models of Griffith's theory has been proposed in [8] with the name *eigenfracture*. The approach is based on a particular set of deformations that cost no local energy and are called *eigendeformation*, see [9]. This approach presents two main issues. First, it is possible to formulate an energy functional characterized by the strain energy depending on the displacement field u and on the eigendeformation $\varepsilon^\star$. Second, the fracture energy is scaled by a numerical parameter and it is considered proportional to the volume of a particular neighborhood of the support of the eigendeformation field. This neighborhood can approximately be compared to the length scale found in other damage models like the phase-field approach or the nonlocal microplane damage model, e.g. see [10] and [11].

The eigenerosion method stems from the eigenfracture scheme based on element erosion. Introduced by [12], it is characterized by the restriction of element erosion in a binary sense: it can be equal to 0, if the element is eroded or 1 in case of fully elastic behavior. In the framework of Finite Element Analysis (FEA), this method models fracture propagation as successive failing elements as soon as their attendant elastic energy release exceeds the corresponding dissipated fracture energy. The eroded elements lose the bearing capacity and, thus, their stiffness matrix is reduced to zero. As proved by [8] and [12], the accuracy and convergence of the eigenerosion approach are comparable to that of other more complex numerical fracture schemes characterized by higher computational cost, e.g. see [13, 14, 15, 16]. In addition, the convergence of this approach to the Griffith fracture model for a reducing mesh size is known *a priori*, see [8].

In [17], the failure of concrete in tension and compression is considered separately for metaconcrete. An alternative way to separate tensile and compressive behavior is the focus of the present work. As the fracture phenomenon is related to tensile loading, distinguishing the latter one, would require the understanding of the fracture process at the crack tip. Illustrative examples, where the method might apply, are out of the area of static

Please cite this document as: Stochino, F., Qinami, A., Kaliske, M. (2017). Eigenerosion for static and dynamic brittle fracture. Engineering Fracture Mechanics, DOI:10.1016/j.engfracmech.2017.05.025

and dynamic crack propagation. The alternation between tensile and compression waves at the crack would cause opening and closing of the crack, respectively. If the stiffness matrix of the eroded elements is reduced to zero, the presence of compression induces penetration of elements coming from opposite crack faces. This problem can be overcome, if the compressive resistance of the eroded element is still kept. The procedure is carried out by applying a spectral decomposition of the strain field into compression and tension. The same procedure is applied in case of the phase-field model presented in [18].

The organization of this paper is as follows: in Section 2, the underlying theory necessary for developing the proposed approach is explained; the variational formulation of the Griffith approach to fracture mechanics and the numerical discretization are presented. Section 3 reports the algorithmic structure and characteristics. Numerical quasi-static and dynamic examples are shown and commented in Section 4. Finally, in Section 5 conclusive remarks are given.

A full list of symbols used is provided for the reader's convenience.

Symbol	Definition
A_e	crack area attendant to erosion of element e
C	crack set
C_ϵ	crack neighborhood
$\|C\|$	area of the crack
$\|C_\epsilon\|$	volume of the crack neighborhood
$\mathbb{C}$	elasticity tensor
C_1	numerical parameter
d	erosion parameter
E	potential energy
E_c	concrete Young's modulus
E_e	extended elastic energy
E_g	global elastic energy functional
$\mathbf{f}$	load vector
F	energy dissipation functional
F_ϵ	regularized extended elastic energy
G	energetic force acting on the crack front
G_c	critical energy release rate
h	smallest element size

Please cite this document as: Stochino, F., Qinami, A., Kaliske, M. (2017). Eigenerosion for static and dynamic brittle fracture. Engineering Fracture Mechanics, DOI:10.1016/j.engfracmech.2017.05.025

$\mathbf{I}$	second order identity tensor
$\mathbf{K}$	global stiffness matrix
$\mathbf{K}_e$	element stiffness matrix
$\mathbf{n}$	unit outward normal to the crack boundary
N_ϵ^e	element e neighborhood
$\mathbb{P}$	fourth order projection tensor
P	applied dynamic force
t	time
$\mathbf{T}$	applied traction
$\mathbf{u}$	displacement field
u_v	applied vertical displacement
v	crack front velocity
W	elastic strain energy
β,γ	Newmark method parameters
Γ	traction prescribed boundary
δ	opening displacement field
δ_c	generic distribution function
ΔE_e	elemental energy releases
Δt	time step
$\boldsymbol{\varepsilon}$	strain field
$\boldsymbol{\varepsilon}^\star$	eigendeformation field
ϵ	regularization parameter
λ	first Lamé's elastic parameter
ρ	material density
μ	shear modulus
$\boldsymbol{\sigma}$	stress field
Ψ	elastic energy density
Ω	body volume
$CMOD$	crack mouth opening dispalcement
$DENS$	double edged notched specimen
FEA	finite element analysis
FEM	finite element method
nEG_e	net energy gain
PQ	priority queue
TOL	tolerance parameter
$SHPB$	Split-Hokpinson pressure bar

Please cite this document as: Stochino, F., Qinami, A., Kaliske, M. (2017). Eigenerosion for static and dynamic brittle fracture. Engineering Fracture Mechanics, DOI:10.1016/j.engfracmech.2017.05.025

2. Theoretical description

2.1. Variational formulation

As a dissipative and irreversible process, fracture can be described by a consistent energetic formulation. From this, one can conclude that if an elastic body with a crack is considered, its elastic energy dissipated in the form of fracture energy at the crack tip can only increase or remain unchanged. The variational formulation of fracture for linear elasticity described in this section is taken from [8, 12]. In order to present this approach more from an engineering rather then a mathematical point of view, the notation used in the following is in agreement with [12]. This description is started by considering an elastic body with a three-dimensional volume Ω, a crack set labeled by C and its boundary, as shown in Fig. 1.

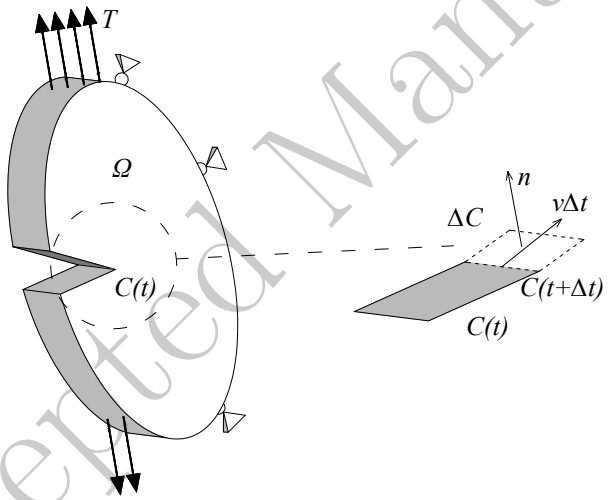

Figure 1: Crack in a solid body. Ω represents the body volume, $\mathbf{T}$ denotes the applied traction, $C(t)$ is the crack set at time instant t, its variation is denoted as ΔC, $\mathbf{n}$ represents the unit outward normal to the boundary and v is the crack front velocity

Under the action of external loads, prescribed displacements or body forces, the body is deformed and its potential energy at a certain time t can be expressed by

$$E(\mathbf{u}, C, t) = \int_{\Omega \setminus C} W(\boldsymbol{\varepsilon}(\mathbf{u}))\, dV - \int_{\Gamma} \mathbf{T} \cdot \mathbf{u}\, dS \quad , \tag{1}$$

Please cite this document as: Stochino, F., Qinami, A., Kaliske, M. (2017). Eigenerosion for static and dynamic brittle fracture. Engineering Fracture Mechanics, DOI:10.1016/j.engfracmech.2017.05.025

where $\Omega \backslash C$ and Γ respectively represent the part of the volume without cracks and the part of the boundary in which the traction loads are prescribed, W is the elastic strain energy due to displacements, $\mathbf{T}$ denotes the applied traction and $\mathbf{u}$ is the displacement field. The strain operator of linear elasticity $\boldsymbol{\varepsilon}(\mathbf{u})$ is defined as

$$\boldsymbol{\varepsilon}(\mathbf{u}) = \frac{1}{2}\left(\nabla \mathbf{u} + (\nabla \mathbf{u})^T\right) \quad . \tag{2}$$

At any time t, the equilibrium conditions can be enforced by the minimization of the potential energy (1).

An increase of the load from time step t to $t + \Delta t$ advances the crack $C(t)$ to $C(t + \Delta t)$. In addition, if $\mathbf{n}$ denotes the unit outward normal to the boundary, irreversibility and contact constraints are given as

$$C(t) \subset C(t + \Delta t) \quad \text{and} \quad [[\mathbf{u}]] \cdot \mathbf{n} \geq 0 \quad . \tag{3}$$

The definition of the energetic force acting on the crack front $G(\mathbf{n})$ can be easily obtained after the definition of the released elastic energy

$$G(\mathbf{n}) = \lim_{\Delta t \to 0} \frac{\partial W(\boldsymbol{\varepsilon}(\mathbf{u}))}{\partial \boldsymbol{\varepsilon}(\mathbf{u})} \mathbf{n} \cdot [[\mathbf{u}(t + \Delta t)]] \quad , \tag{4}$$

and its time derivative, see [12].

If G_c denotes the critical energy release rate and v is the crack front velocity, it is possible to express the Griffith's crack propagation and arrest criteria with the following set of equations

$$\begin{cases} G - G_c \leq 0 \quad , \\ v \geq 0 \quad , \\ (G - G_c)v = 0 \quad . \end{cases} \tag{5}$$

Considering the above mentioned hypothesis, the crack propagation problem can be reduced to minimization of the energy dissipation functional

$$F(\mathbf{u}, C, t) = E(\mathbf{u}, C, t) + G_c \left|C\right| \quad , \tag{6}$$

with $|C|$ being the area of the crack.

The crack path is obtained by minimizing Eq. (6) with respect to both the displacement field $\mathbf{u}$ and the crack set C. In other words, crack propagation depends on the balance between the elastic energy that can advance the

Please cite this document as: Stochino, F., Qinami, A., Kaliske, M. (2017). Eigenerosion for static and dynamic brittle fracture. Engineering Fracture Mechanics, DOI:10.1016/j.engfracmech.2017.05.025

fracture process and the fracture energy, proportional to the crack-area, that opposes this advancement.

As yet, the continuous variational formulation is purely mathematical. In order to approximate the problem numerically, one approach is to reformulate it in terms of eigendeformations $\boldsymbol{\varepsilon}^\star$. To this regard, the extended elastic energy is defined

$$E_e(\mathbf{u}, \boldsymbol{\varepsilon}^\star, t) = \int_\Omega W(\boldsymbol{\varepsilon}(\mathbf{u}) - \boldsymbol{\varepsilon}^\star(\delta))\, dV - \int_\Gamma \mathbf{T} \cdot \mathbf{u}\, dS \quad . \tag{7}$$

The definition of eigendeformation is obtained by means of $\delta = [[\mathbf{u}]]$, which is the opening displacement field across C and its unit normal $\mathbf{n}$

$$\varepsilon^\star_{ij} = \frac{1}{2}\left(\delta_i n_j + \delta_j n_i\right)\delta_C \quad , \tag{8}$$

where δ_C represents a given distribution over the crack set C. This representation of eigendeformation allows the displacement field to develop jumps. Schmidt et al. [8] presented a convergent element erosion (eigenerosion) scheme based on the regularization of the extended energy (Eq. (7))

$$F_\epsilon(\mathbf{u}, \varepsilon^\star, t) = \int_\Omega W(\boldsymbol{\varepsilon}(\mathbf{u}) - \varepsilon^\star(\delta))\, dV - \int_\Gamma \mathbf{T} \cdot \mathbf{u}\, dS + G_c \frac{|C_\epsilon|}{2\epsilon} \quad , \tag{9}$$

where ϵ is a small numerical parameter with the unit of length, C is the support of the eigendeformation field (an approximation to the crack set) and C_ϵ denotes the set of points characterized by a distance less or equal to ϵ from C. The volume of C_ϵ is labelled by $|C_\epsilon|$ and it can represent a volume of damaged materials. In [8], the proof of Γ-convergence of Eq. (9) to Eq. (6), when $\epsilon \to 0$, is shown.

2.2. Element formulation

In [18], a rate-independent phase-field problem is investigated, where a spectral decomposition of the strain field leads to a possible separation of the tensile and compressive behavior. Based on that approach, the following element formulation is described in the context of FEM. If one considers an elastic isotropic solid with a set of cracks, it is possible to represent the degradation of the elastic energy functional by means of a binary numerical parameter d, which can be defined as

$$\begin{cases} d = 0 : & fracture \quad , \\ d = 1 : & no\, fracture \quad . \end{cases} \tag{10}$$

Please cite this document as: Stochino, F., Qinami, A., Kaliske, M. (2017). Eigenerosion for static and dynamic brittle fracture. Engineering Fracture Mechanics, DOI:10.1016/j.engfracmech.2017.05.025

Thus, the global elastic energy functional is defined by

$$E_g(\mathbf{u}, d) = \int_\Omega \Psi(\boldsymbol{\varepsilon}(\mathbf{u}), d) dV \quad . \tag{11}$$

The energy function Ψ represents the elastic energy density stored in the body. This energy functional can be splitted into its positive and negative parts corresponding to tension and compression, respectively, as follows

$$\Psi(\boldsymbol{\varepsilon}(\mathbf{u}), d) = d\ \Psi^+(\boldsymbol{\varepsilon}(\mathbf{u})) + \Psi^-(\boldsymbol{\varepsilon}(\mathbf{u})) \quad , \tag{12}$$

where

$$\Psi^+(\boldsymbol{\varepsilon}) = \lambda \frac{\langle \mathrm{tr}(\boldsymbol{\varepsilon}) \rangle_+^2}{2} + \mu\ \mathrm{tr}(\boldsymbol{\varepsilon}_+^2) \quad . \tag{13}$$

$$\Psi^-(\boldsymbol{\varepsilon}) = \lambda \frac{\langle \mathrm{tr}(\boldsymbol{\varepsilon}) \rangle_-^2}{2} + \mu\ \mathrm{tr}(\boldsymbol{\varepsilon}_-^2) \quad , \tag{14}$$

The bracket operators $\langle x \rangle_+ = (x + |x|)/2$ and $\langle x \rangle_- = (x - |x|)/2$ have to be considered. The positive $\boldsymbol{\varepsilon}_+$, and the negative $\boldsymbol{\varepsilon}_-$ can be calculated by solving an eigenvalue problem for the strain tensor $\boldsymbol{\varepsilon}$. Thus, if ε^i represents the i-th eigenvalue and and $\mathbf{n}^i$ its corresponding eigenvector, the spectral decomposition of the strain tensor $\boldsymbol{\varepsilon}$ is expressed by

$$\boldsymbol{\varepsilon}_+ = \sum_{i=1}^{n} \langle \varepsilon^i \rangle_+ \mathbf{n}^i \otimes \mathbf{n}^i \quad , \tag{15}$$

$$\boldsymbol{\varepsilon}_- = \sum_{i=1}^{n} \langle \varepsilon^i \rangle_- \mathbf{n}^i \otimes \mathbf{n}^i \quad . \tag{16}$$

The stress tensor can be defined by means of the constitutive equation

$$\boldsymbol{\sigma} = \partial_{\boldsymbol{\varepsilon}} \Psi(\boldsymbol{\varepsilon}, d). \tag{17}$$

Introducing the two elastic parameters λ and μ, it is also possible to highlight the contribution of the positive and negative strains

$$\boldsymbol{\sigma} = d\ \left(\lambda\ \langle \mathrm{tr}(\boldsymbol{\varepsilon}) \rangle_+\ \mathbf{I} + 2\mu\, \boldsymbol{\varepsilon}_+ \right) + \lambda\ \langle \mathrm{tr}(\boldsymbol{\varepsilon}) \rangle_-\ \mathbf{I} + 2\mu\, \boldsymbol{\varepsilon}_- \quad . \tag{18}$$

Please cite this document as: Stochino, F., Qinami, A., Kaliske, M. (2017). Eigenerosion for static and dynamic brittle fracture. Engineering Fracture Mechanics, DOI:10.1016/j.engfracmech.2017.05.025

Consequently, the stresses can be obtained as

$$\begin{aligned} \boldsymbol{\sigma}_+ &= \lambda \, \langle \mathrm{tr}(\boldsymbol{\varepsilon}) \rangle_+ \, \mathbf{I} + 2\mu \, \boldsymbol{\varepsilon}_+ \quad , \\ \boldsymbol{\sigma}_- &= \lambda \, \langle \mathrm{tr}(\boldsymbol{\varepsilon}) \rangle_- \, \mathbf{I} + 2\mu \, \boldsymbol{\varepsilon}_- \quad . \end{aligned} \tag{19}$$

The elasticity tensor then is given as

$$\mathbb{C} = \frac{\partial \boldsymbol{\sigma}}{\partial \boldsymbol{\varepsilon}} = d \, \frac{\partial \boldsymbol{\sigma}_+}{\partial \boldsymbol{\varepsilon}} + \frac{\partial \boldsymbol{\sigma}_-}{\partial \boldsymbol{\varepsilon}} \quad , \tag{20}$$

$$\mathbb{C} = d \, \mathbb{C}_+ + \mathbb{C}_- \quad , \tag{21}$$

with

$$\mathbb{C}_+ = \frac{1}{2} \lambda \, \mathbf{I} \otimes (\mathbf{I} + \mathrm{sgn}(\mathrm{tr}(\boldsymbol{\varepsilon})) \, \mathbf{I}) + 2 \, \mu \, \mathbb{P}_+ \quad , \tag{22}$$

and

$$\mathbb{C}_- = \frac{1}{2} \lambda \, \mathbf{I} \otimes (\mathbf{I} - \mathrm{sgn}(\mathrm{tr}(\boldsymbol{\varepsilon})) \, \mathbf{I}) + 2 \, \mu \, \mathbb{P}_- \quad , \tag{23}$$

with the fourth order tensors $\mathbb{P}_+ = \partial \boldsymbol{\varepsilon}_+ / \partial \boldsymbol{\varepsilon}$ and $\mathbb{P}_- = \partial \boldsymbol{\varepsilon}_- / \partial \boldsymbol{\varepsilon}$.

It is meaningful to highlight as a characteristic of this work, as shown in Eq. (18), that the degradation parameter d is affecting only the tensile part limiting the erosion effect to this partial reduction of element stiffness.

3. Algorithmic implementation of enhanced eigenerosion

The implementation of eigenerosion is mainly a postprocessing procedure. This implementation is done using a displacement based finite element code. In Fig. 2, a schematic representation of the method is given in the form of a flowchart.

Please cite this document as: Stochino, F., Qinami, A., Kaliske, M. (2017). Eigenerosion for static and dynamic brittle fracture. Engineering Fracture Mechanics, DOI:10.1016/j.engfracmech.2017.05.025

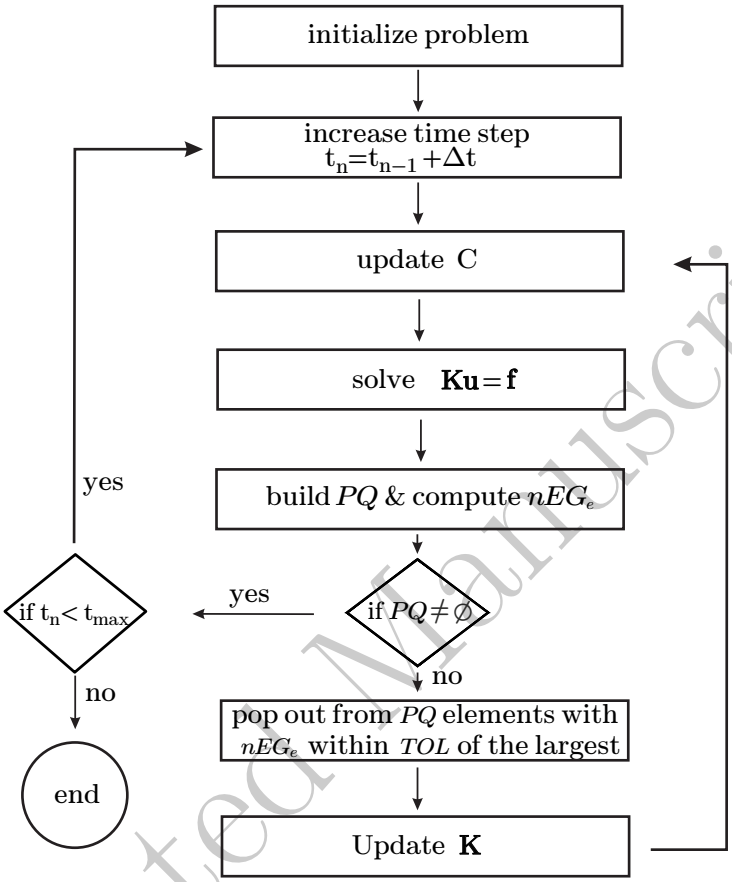

Figure 2: Eigenerosion algorithm flowchart.

The procedure starts with the linear elastic solution for a given time step t_n. All the eroded elements are part of a crack list denoted with C. In a further step, each element, not in the crack list C, is tested for a possible erosion. Indeed, once the elastic problem is solved, the displacements for a certain time-step $\mathbf{u}$ are known and the balance of energy can be calculated. This means that the elastic energy released for the erosion of one element $-\Delta E_e$ is compared to the fracture energy $G_c \cdot \Delta A_e$ related to this particular element. The difference between these two energies is called the *net energy gain* for each element and is given as

$$nEG_e = -\Delta E_e - G_c \cdot \Delta A_e \quad . \tag{24}$$

Please cite this document as: Stochino, F., Qinami, A., Kaliske, M. (2017). Eigenerosion for static and dynamic brittle fracture. Engineering Fracture Mechanics, DOI:10.1016/j.engfracmech.2017.05.025

If the elastic energy for the element in study exceeds the fracture one ($nEG_E > 0$), this element is added to a priority queue, PQ. This priority queue contains an ordered list of elements in which the first position is occupied by the element with the largest nEG_e. The elements that are part of the PQ can be eroded. Actually, as reported in [12], in order to avoid numerically biased advances of the crack, it is necessary to allow groups of elements with similar net energy gains to be eroded at the same iteration. This can be done popping out from the PQ all the elements that have nEG_e within a certain tolerance TOL of the first one. In this way, the amount of elements from PQ that will be eroded at each iteration is user defined through the TOL parameter value. These elements are added to the crack list C and their stiffness will be later reduced. Thus, after the erosion, the global stiffness $\mathbf{K}$ is modified and it is necessary to enforce again the equilibrium condition

$$\mathbf{K}\mathbf{u} = \mathbf{f} \quad , \tag{25}$$

where $\mathbf{f}$ is the external load array. Fulfilling the new equilibrium conditions denotes another solution for the same time step t_n. This means, the above mentioned process will be repeated until the priority queue PQ will be empty. When this condition is fulfilled, it is possible to pass to the next time step and increase the load.

In [12], the stiffness of an eroded element is completely set to zero. Instead, in this work, an enhanced approach is assumed. Considering a brittle material like concrete that presents a not symmetric constitutive law (e.g. the compressive behavior is very different from the tensile one), it is useful to separate the contribution to the element's elastic stiffness matrix $\mathbf{K}_e$ of the tensile (positive) constitutive tensor $\mathbf{K}_e^+$ and of the compressive (negative) one $\mathbf{K}_e^-$. Considering also the variable d, which is useful to model the erosion, this writes

$$\mathbf{K}_e = d\,\mathbf{K}_e^+ + \mathbf{K}_e^- . \tag{26}$$

In this way, if an element is subjected to erosion, it is possible to account for the stress degradation only in tension, keeping a residual stiffness for compressive stress. This characteristic can be of large relevance for dynamic problems in which the stress wave propagation can be biased by a full erosion of the element stiffness. Instead, the reduction of the tensile part $\mathbf{K}_e^+$ can easily avoid any penetration problem due to stress wave propagation through fracture. The separation of the two parts of the elasticity tensor which build

Please cite this document as: Stochino, F., Qinami, A., Kaliske, M. (2017). Eigenerosion for static and dynamic brittle fracture. Engineering Fracture Mechanics, DOI:10.1016/j.engfracmech.2017.05.025

the corresponding stiffness matrixes of Eq. (26), is presented in Section 2.2, see [18] and [19] for a more mathematical description of the approach.

3.1. Elemental energy releases

A key point of the eigenerosion algorithm is the evaluation of the element energy release. It has been proved that it is possible to provide a first order estimation of this quantity in accordance with the asymptotic formulation for the energy release rate attendant to notch-tip erosion, see [20], [21].

If the global stiffness matrix of a linear elastic body is $\mathbf{K} + \Delta\mathbf{K}_e$, where $\mathbf{K}$ represents the global stiffness matrix without the element e and $\Delta\mathbf{K}_e = \Delta\mathbf{K}_e^+ + \Delta\mathbf{K}_e^-$ is the stiffness matrix of element e, the energy released from its erosion can be expressed as the difference in the total potential energy

$$\begin{aligned} -\Delta E_e =& \frac{1}{2}\mathbf{u}^T \left(\mathbf{K} + \Delta\mathbf{K}_e\right)\mathbf{u} - \mathbf{f}^T\mathbf{u} \\ & -\frac{1}{2}(\mathbf{u}+\Delta\mathbf{u})^T \left(\mathbf{K} + \Delta\mathbf{K}_e^-\right)(\mathbf{u}+\Delta\mathbf{u}) - \mathbf{f}^T(\mathbf{u}+\Delta\mathbf{u}) \quad , \end{aligned} \tag{27}$$

where $\mathbf{u}$ and $\mathbf{u}+\Delta\mathbf{u}$, respectively, denote the displacement field before and after the erosion.

Enforcing the equilibrium conditions before and after the erosion, one can write

$$\left(\mathbf{K} + \Delta\mathbf{K}_e\right)\mathbf{u} = \mathbf{f}^T \quad , \tag{28}$$

$$\left(\mathbf{K} + \Delta\mathbf{K}_e^-\right)(\mathbf{u}+\Delta\mathbf{u}) = \mathbf{f}^T \quad . \tag{29}$$

It is possible to simplify Eq. (27) to the quadratic form

$$-\Delta E_e = \frac{1}{2}\mathbf{u}^T \left(\Delta\mathbf{K}_e^+ + \Delta\mathbf{K}_e^+(\mathbf{K}+\Delta\mathbf{K}_e)^{-1}\Delta\mathbf{K}_e^+\right)\mathbf{u} \quad . \tag{30}$$

In order to reduce the computational effort necessary to evaluate $(\mathbf{K} + \Delta\mathbf{K}_e)^{-1}$, it is possible to approximate Eq. (30) with its first order expansion

$$-\Delta E_e \sim \frac{1}{2}\mathbf{u}^T \left(\Delta\mathbf{K}_e^+\right)\mathbf{u} \quad . \tag{31}$$

Eq. (31) represents a very efficient approach because it is explicit (both displacements field $\mathbf{u}$ and the positive part of the element stiffness matrix $\mathbf{K}_e^+$ are known) and its computational cost is very low.

Please cite this document as: Stochino, F., Qinami, A., Kaliske, M. (2017). Eigenerosion for static and dynamic brittle fracture. Engineering Fracture Mechanics, DOI:10.1016/j.engfracmech.2017.05.025

3.2. Fracture energy and ϵ-neighborhood definition

The other key-point in the eigenerosion algorithm is the computation of the fracture energy. In particular, it is based on the product between the material characteristic critical energy release rate G_c and the increment of the crack area attendant to erosion ΔA_e. The crack set C is the union of all eroded elements. The corresponding ϵ-neighborhood of C is identified by C_ϵ and is the set of elements, whose barycenters have a distance smaller than ϵ from any of the barycenters of the eroded elements belonging to C.

Thus, if one assumes that the ϵ neighborhood of element e, N^e_ϵ represents, as above mentioned, the set of all elements, whose barycenter have a distance smaller than ϵ from the element e barycenter, the increment of the crack area attendant to the erosion of element e is

$$\Delta A_e = \frac{\|(C \cup N^e)_\epsilon \backslash C_\epsilon\|}{2\epsilon}, \tag{32}$$

where $(C \cup N^e)$ is the new crack set after the erosion of element e and '\' denotes difference. So, $\|(C \cup N^e)_\epsilon \backslash C_\epsilon\|$ represents the volume of the elements included in the e element neighborhood N^e_ϵ that are not present in the old crack neighborhood C_ϵ, see Fig. 3.

Please cite this document as: Stochino, F., Qinami, A., Kaliske, M. (2017). Eigenerosion for static and dynamic brittle fracture. Engineering Fracture Mechanics, DOI:10.1016/j.engfracmech.2017.05.025

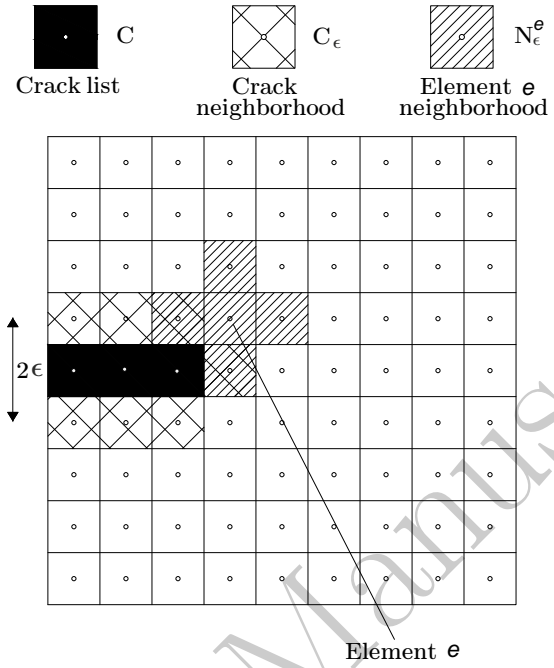

Figure 3: Scheme of ϵ-neighborhood construction.

Then, in order to evaluate ΔA_e, it is sufficient to compare the element e neighborhood N_ϵ^e with the crack neighborhood C_ϵ. All elements present in N_ϵ^e and not in C_ϵ or C give a contribution to ΔA_e.

The value of ϵ, which has the dimension of length, is a crucial aspect of the procedure. In order to have convergence of the numerical procedure, it must tend to zero more slowly than the mesh size, see [8].

In this work, following the suggestions in [12], the value of ϵ has been defined by

$$\epsilon = C_1 h \quad , \tag{33}$$

where C_1 is a numerical coefficient larger than one and h is the smallest element size in the mesh.

The value of C_1 cannot be too large. It is clear that the maximum value of ϵ must be limited by the total body size. Indeed, if C_1 is too big, every element will be in every element neighborhood yielding $\Delta A_e = 0$ and, consequently, avoiding any erosion.

In this work, the value of C_1 has been chosen between 1 and 10 for each numerical example considering the specific geometry of the problem.

Please cite this document as: Stochino, F., Qinami, A., Kaliske, M. (2017). Eigenerosion for static and dynamic brittle fracture. Engineering Fracture Mechanics, DOI:10.1016/j.engfracmech.2017.05.025

4. Numerical Examples

In order to prove the efficacy of the approach, a number of numerical examples have been chosen. Among these model problems, two static and two dynamic cases have been included, one two-dimensional and one three-dimensional, respectively. The main quantity, that has been studied, is mostly the crack shape predicted by eroded elements in comparison to other methods from the literature or to experimental data. Apart from that, other relevant quantities will be commented.

4.1. Double edged notched specimen

The Double Edge Notched Specimen (DENS) is thoroughly studied in [22] as part of mixed mode fracture tests for concrete structures. The specimen geometry and the applied loading are given in Fig. 4. The experiment starts with the application of the load H as a shear load at the sides until it reaches a certain level H_0. After this point, the horizontal load is kept constant and a displacement in vertical direction at the top and at the bottom of the specimen are applied. The simulation presented here differs from the original version of [22] in the sense that the three-dimensional specimen is modeled as a two-dimensional test.

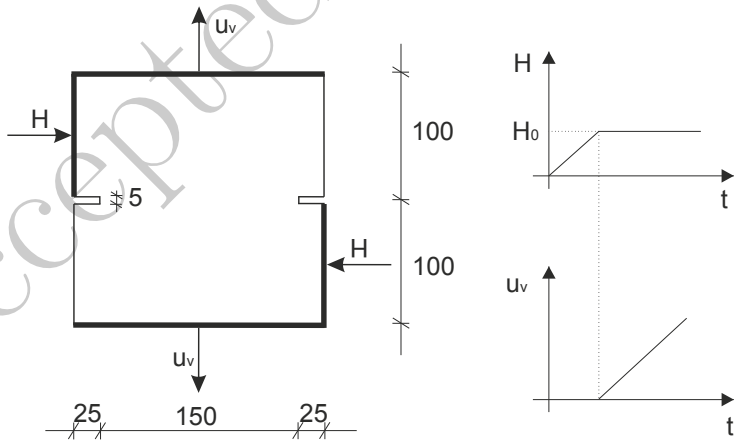

Figure 4: Specimen geometry and loading.

The following parameters have been chosen: Lamé coefficients $\lambda = 20.2$ GPa, $\mu = 13.46$ GPa; critical energy release rate $G_c = 51$ N/m; $C_1 = 2.2$

Please cite this document as: Stochino, F., Qinami, A., Kaliske, M. (2017). Eigenerosion for static and dynamic brittle fracture. Engineering Fracture Mechanics, DOI:10.1016/j.engfracmech.2017.05.025

and $TOL = 0.7$. This type of loading develops two cracks starting from the two notches in opposite directions. For this specific example, the load is chosen as $H_0 = 0.1$ kN and incremental displacement of $\Delta u_v = 0.003$ mm. The geometry is discretized by 4936 elements. In Fig. 5 a), the crack development for this specimen approximated with the eigenerosion approach is shown and in Fig. 5 b), the experimental results for one load case, taken from [22], are shown.

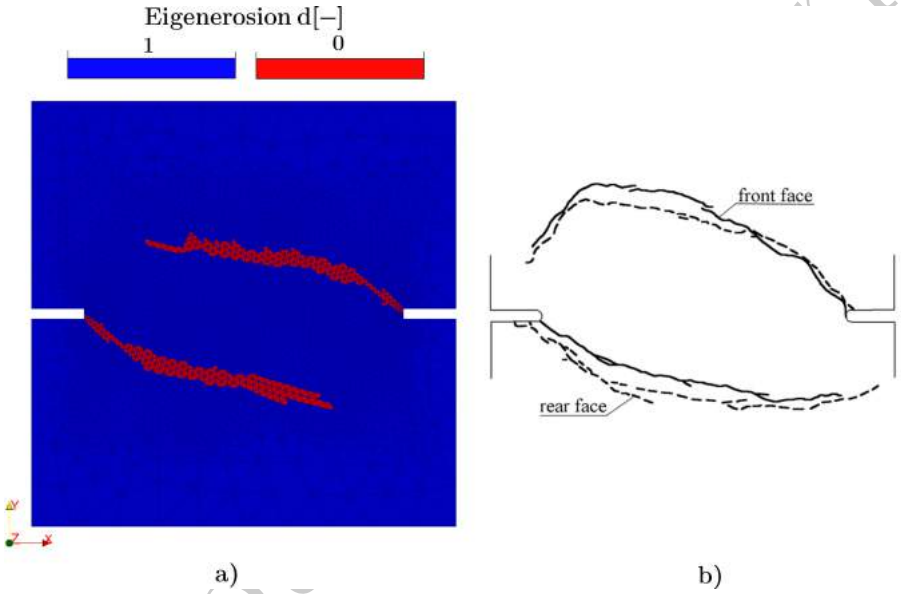

Figure 5: Crack development starting from two opposite notches: a) eigenerosion; b) experimental results, taken from [22].

The crack shapes satisfactorily match the experimental results. Having the three-dimensional specimen modeled in two-dimensions leads to some differences in results from the fracture point of view. In three-dimensional case, the neighborhood of each element has a larger volume then the one of the two-dimensional case. This would mean that the fracture resistance is higher and one would need higher elastic energy to erode one element given that the loading, boundary conditions and eigenerosion parameters are kept unchanged. Thus, a quantitative comparison to the experimental results is not relevant in this case.

Please cite this document as: Stochino, F., Qinami, A., Kaliske, M. (2017). Eigenerosion for static and dynamic brittle fracture. Engineering Fracture Mechanics, DOI:10.1016/j.engfracmech.2017.05.025

4.2. Prismatic torsion test

The torsion fracture test of notched concrete beams developed by Barr and Brokenshire [23], [24] is an interesting quasi-static benchmark test for the eigenerosion algorithm. In the above mentioned works, several kinds of beams are tested (notched and un-notched, prismatic and cylindrical) in order to establish the elastic properties and torsional shear strength of concrete. Some numerical analyses and experimental details can also be found in [25].

In particular, in this paper, the case shown in Fig. 6 is considered. The specimen dimensions are characterized by 100 × 100 mm cross-section, 400 mm length. The torsional load is applied by means of a steel jacket located at both beam ends. The feedback for the loading rate has been given by a clip gauge at the notch mouth.

The concrete elastic modulus, E_c, is measured equal to 34.9 kN/mm^2, while its critical energy release rate is 73 N/m.

The eigenerosion algorithm is applied to a mesh of 4592 four-noded tetrahedral elements considering the concrete elastic modulus E_c equal to 35 kN/mm^2, $G_c = 70$ N/m, $C_1 = 3.35$, $TOL = 0.6$. The concrete is represented as a purely linear elastic material with the above mentioned characteristics.

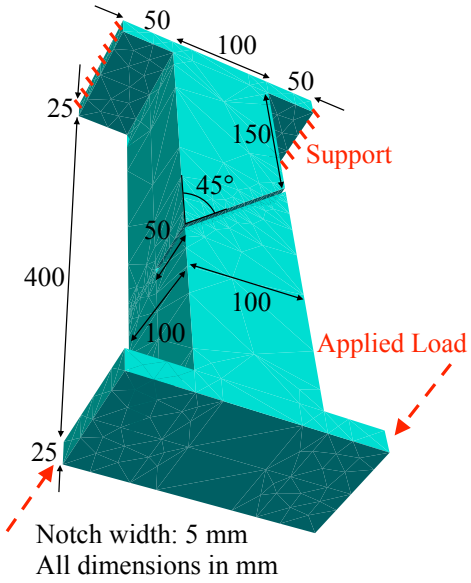

Figure 6: Torsion test on notched prismatic beam, geometry and boundary conditions, extracted from [25].

Please cite this document as: Stochino, F., Qinami, A., Kaliske, M. (2017). Eigenerosion for static and dynamic brittle fracture. Engineering Fracture Mechanics, DOI:10.1016/j.engfracmech.2017.05.025

Fig. 7 shows several views of the full crack development at the end of the simulation.

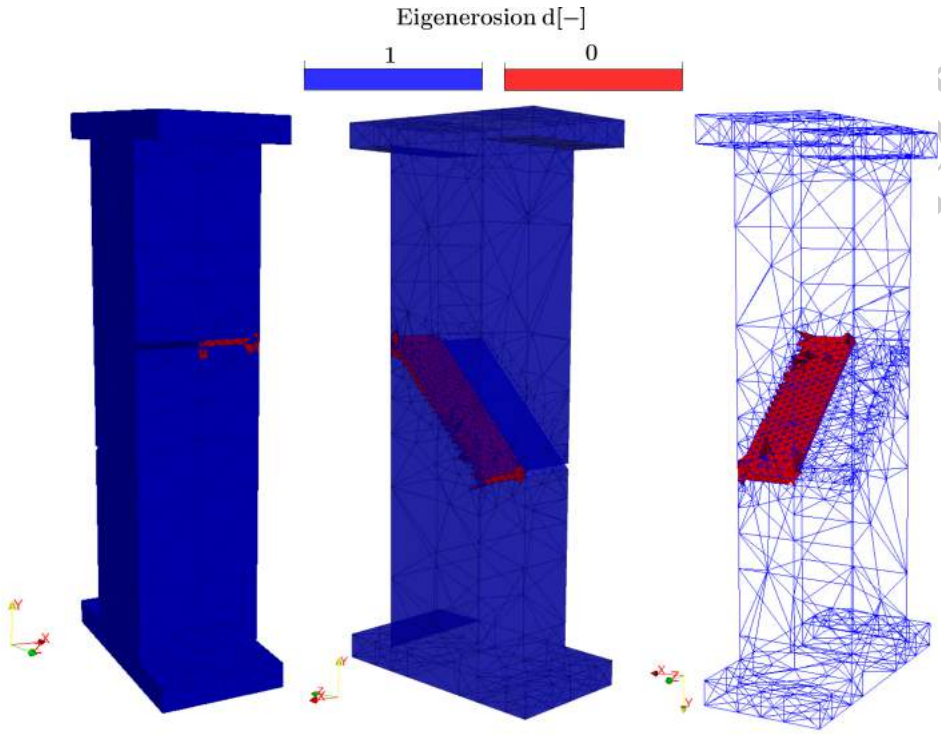

Figure 7: Crack development for the prismatic beam under torsion.

Also the Crack Mouth Opening Displacement (CMOD) as function of load has been recorded during the experimental test and determined by FEM, see Fig. 8. The eigenerosion simulation compares quite well to the experimental results and to the numerical simulation presented in [25].

Please cite this document as: Stochino, F., Qinami, A., Kaliske, M. (2017). Eigenerosion for static and dynamic brittle fracture. Engineering Fracture Mechanics, DOI:10.1016/j.engfracmech.2017.05.025

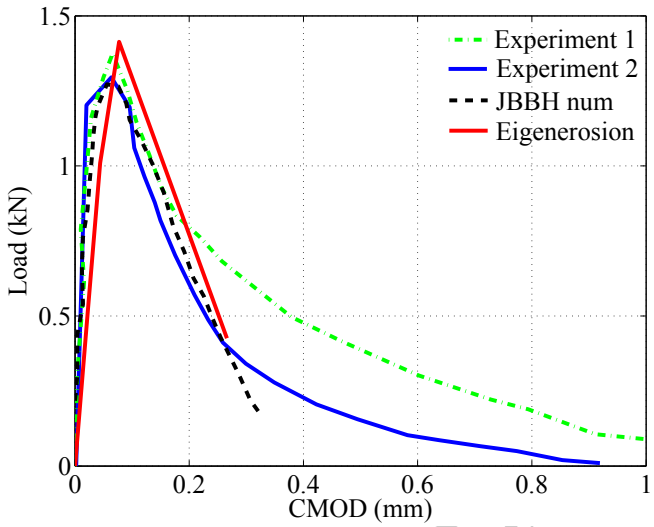

Figure 8: Load-CMOD relations for eigenerosion model, numerical and experimental results, see Jefferson et al. [25].

From the graphs in Fig. 8, the brittleness of the method can be observed. While the experimental curves show softening of the material, the eigenerosion approach prescribes a rapid evolvement of the crack until two separate bodies are created, depicted by the end of the red curve.

4.3. Crack branching simulation

A first example to test the method in the dynamic case is a crack branching simulation in a wave propagation problem. This example is studied in [26], where different damage models are applied and, in [27], where a phase-field and material force approach are tested for this fracture problem. The boundary conditions and load application for this test are shown in Fig. 9.

Please cite this document as: Stochino, F., Qinami, A., Kaliske, M. (2017). Eigenerosion for static and dynamic brittle fracture. Engineering Fracture Mechanics, DOI:10.1016/j.engfracmech.2017.05.025

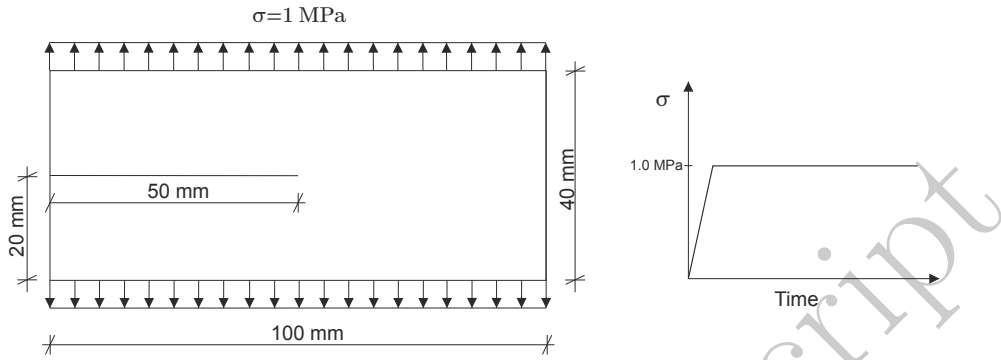

Figure 9: Boundary conditions and load applied to the specimen.

The following parameters have been chosen: Lamé coefficients $\lambda = 8.8$ GPa, $\mu = 13.3$ GPa; material density $\rho = 2450\ \mathrm{kg/m^3}$; critical energy release rate $G_c = 0.1$ N/m; $C_1 = 2.6$ and $TOL = 0.9$. A total number of 16000 quadrilateral elements is used for the mesh. The time step $\Delta t = 0.5\ \mu$s is chosen based on the minimum length of the element and the wave speed in the solid. The Newmark method with parameters $\beta = 0.25$ and $\gamma = 0.7$ is used for time integration. The propagation of the tensile wave at two different times is given in Fig. 10.

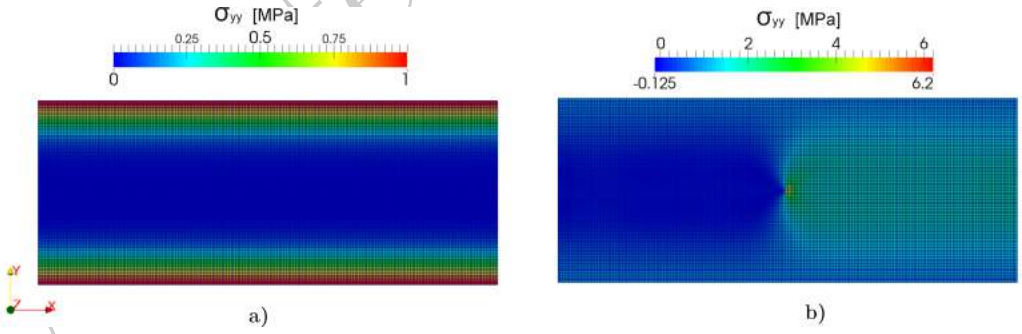

Figure 10: Tensile wave propagation: a) $t = 2.5\,\mu s$; b) $t = 10\,\mu s$. σ_{yy} represents the stress in the vertical direction.

As described in [26], the type of loading for this specimen gives the opportunity to yield branching of the crack. The crack initiates at $t = 11\ \mu$s and branching occurs at $t = 16.5\ \mu$s. During the period of 5.5 μs, the crack

Please cite this document as: Stochino, F., Qinami, A., Kaliske, M. (2017). Eigenerosion for static and dynamic brittle fracture. Engineering Fracture Mechanics, DOI:10.1016/j.engfracmech.2017.05.025

propagates 15 mm with an average speed of 2727 m/s before it branches. Crack development at the end of the simulation modeled by eigenerosion is shown in Fig. 11.

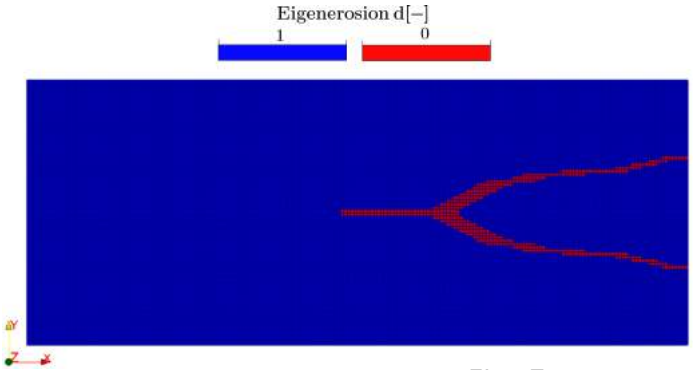

Figure 11: Crack branching in a wave propagation test.

The obtained results are comparable to those given in [26] and [27]. As it is stated in [26], the increase of the tensile strains adjacent to the crack causes crack branching. This phenomenon is noticed also in the presented simulation. The crack starts to propagate as a Mode I crack. Afterwards, observing tensile strains along the x-axis, once they reach a certain peak, branching occurs. For a given loading condition, this peak is depending on the fracture resistance of the structure. A short comment on crack initiation and branching is given in the following remark.

Remark on the results. The critical energy release rate G_c is a material parameter determined experimentally for a specific loading condition. On the other hand, in case of eigenerosion, the fracture resistance is obtained from three parameters, namely, the physical one G_c and the numerical ones C_1, TOL. The combination of these three parameters needs to be calibrated for the desired results. Thus, the selection of these parameters determines not only the crack shape but also initiation and branching time. More practically speaking, changing these parameters leads to a change in the energy release rate for a given structure.

4.4. Split-Hokpinson pressure bar (SHPB) dynamic test

The following simulation is a modified SHPB test. This test is used to determine the dynamic tensile strength of concrete. The setup of this simu-

Please cite this document as: Stochino, F., Qinami, A., Kaliske, M. (2017). Eigenerosion for static and dynamic brittle fracture. Engineering Fracture Mechanics, DOI:10.1016/j.engfracmech.2017.05.025

lation is the one given in [28]. Fig. 12 a) shows a schematic representation of the experimental setup, where three different parts are to be mentioned. It starts with a steel impactor, which hits the incident bar with a given velocity v. A strain gauge is placed on the aluminium incident bar to measure the strains coming from the compressive wave, which travels through this bar. The concrete specimen is situated at the end of the incident bar, which geometry is shown in Fig. 12 b). The compressive wave is transmitted from the bar to the concrete specimen through perfect contact. In order to reduce the computational effort, only the concrete specimen is modeled and a compressive load is applied directly at the top of the specimen. The load is represented through the loading function of Fig. 12 c). The applied loading is then calculated as $\sigma(t) = \sigma_0 \cdot f(t)$.

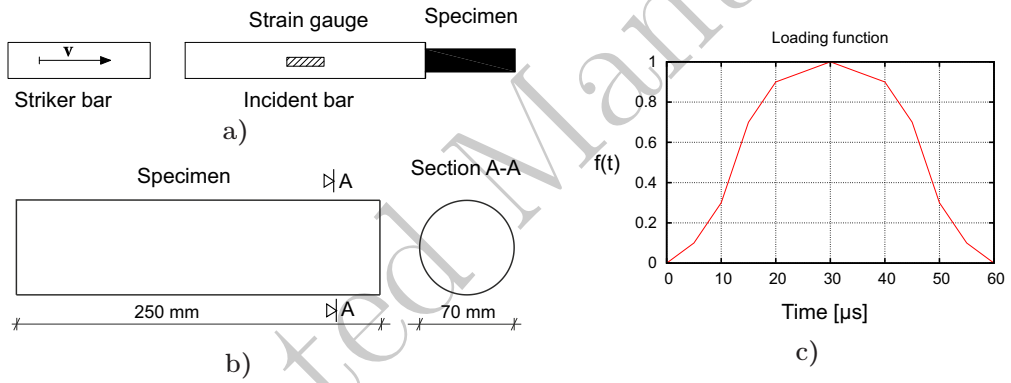

Figure 12: Modified SHPB: a) experiment setup; b) specimen geometry; c) loading function.

The following parameters are chosen: Lamé coefficients $\lambda = 23$ GPa, $\mu = 15.4$ GPa; material density $\rho = 2400$ kg/m^3; critical energy release rate $G_c = 65$ N/m; $C_1 = 2.1$ and $TOL = 0.9$. The Newmark time integration scheme is used with $\Delta t = 1.5$ μs, $\beta = 0.5$ and $\gamma = 0.7$. The applied load is $\sigma_0 = 65$ MPa. The specimen is dicretized with a total number of 11700 solid brick elements. The simulation results for two different times are shown in Fig. 13. A three-dimensional crack development along the specimen is shown in Fig. 14.

Please cite this document as: Stochino, F., Qinami, A., Kaliske, M. (2017). Eigenerosion for static and dynamic brittle fracture. Engineering Fracture Mechanics, DOI:10.1016/j.engfracmech.2017.05.025

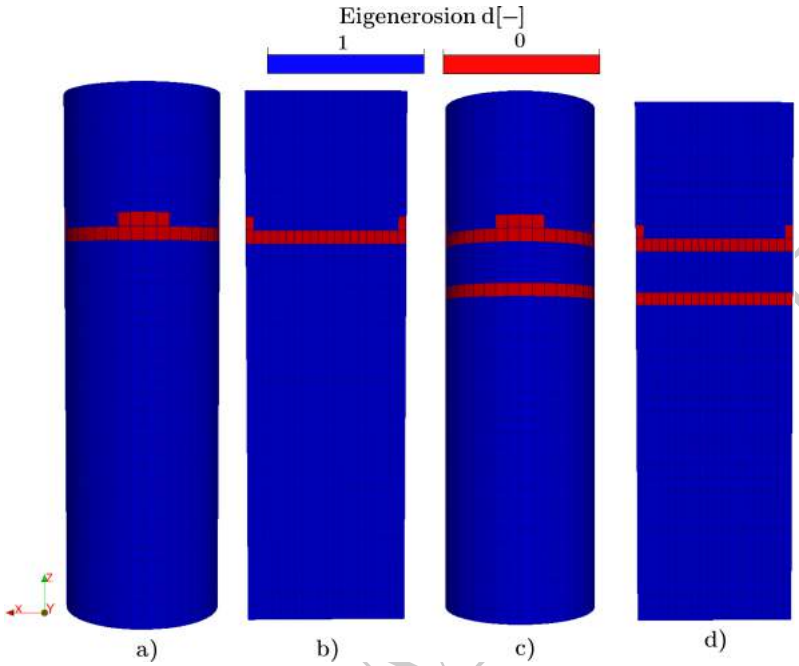

Figure 13: Crack development along the specimen: a) first crack through the specimen at time $t = 99$ μs; b) section cut parallel to longitudinal axis of the specimen at time $t = 99$ μs; c) final step of the simulation at time $t = 100.5$ μs; d) section cut parallel to longitudinal axis of the specimen at time $t = 100.5$ μs.

Please cite this document as: Stochino, F., Qinami, A., Kaliske, M. (2017). Eigenerosion for static and dynamic brittle fracture. Engineering Fracture Mechanics, DOI:10.1016/j.engfracmech.2017.05.025

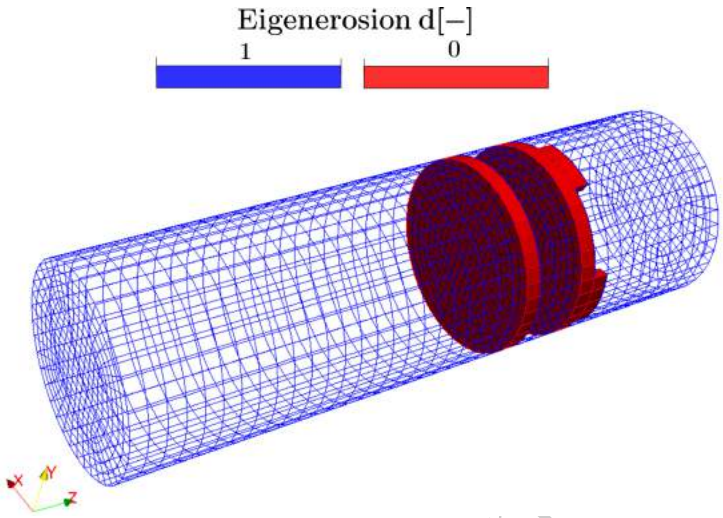

Figure 14: Three-dimensional cack representation

The crack starts after the compressive wave travels along the concrete specimen and it is reflected at its end as a tensile wave. The reflected tensile wave induces the first crack at time $t = 99$ μs, see Fig 13 a) and b). After this time, the simulation is continued until another crack is created, see Fig. 13 c) and d). In [28], several tests with different loading rates are shown and, for the amplitude of the stresses used in this simulation, the eigerosion approach shows a very good agreement with the experimental results. The position and the number of cracks along the specimen are strongly depending on the shape of the applied compressive wave, which is described by the loading function given in Fig. 12 c).

5. Conclusions

In this work, an enhanced version of the eigenerosion algorithm has been presented. It is particularly effective for dynamic problems concerning brittle materials like concrete, glass etc.

The main novelty is the application of spectral decomposition to separate the tensile and compressive part of the stiffness matrix. This procedure is based on an eigenvalue analysis of the strain tensor and allows to apply erosion just to the tensile behavior of the material. In this way, it is possible to avoid penetration for dynamic problems.

Please cite this document as: Stochino, F., Qinami, A., Kaliske, M. (2017). Eigenerosion for static and dynamic brittle fracture. Engineering Fracture Mechanics, DOI:10.1016/j.engfracmech.2017.05.025

The algorithmic details have been discussed carefully highlighting the main characteristics that can be synthesized into an erosion criterion based on the *net energy gain*, which is the difference between the energy released to the system by the erosion of one element and the fracture energy necessary to have the erosion. The elements being a candidate for erosion are sorted in a priority queue based on their *net energy gain*. The ones with the largest values are eroded, their stiffness contribution is reduced and they are added to the crack list C. Once the global stiffness is modified, the elastic linear problem is solved again and the procedure is repeated till no elements have a positive *net energy gain*. Then, the next time step is considered, the loads are updated and the loop is repeated.

One of the main advantages of this approach is its simplicity and the reduced computational effort in comparison to more elaborate models for fracture propagation.

It is worth mentioning that no variational formulation of fracture still exists in literature which accounts for the current energy separation. Nevertheless, comparing the achieved results to those already existing in literature demonstrates a relatively good accuracy of the method. Furthermore, in this publication concrete is considered as purely brittle material while in literature it is mostly studied as quasi-brittle material. The brittleness can also lead to non-realistic crack paths. Considering this fact, new challenges arise for consideration of more realistic material behavior by including inelasticity.

The possible application of this approach is wide-ranging: for example, with little modifications, it is capable of dealing with more complex nonlinear problems for reinforced concrete structures like those presented in [29], quasi-static punching of RC slabs [30] and high rate dynamic loading [31].

Finally, a thorough comparison between eigenerosion and other state of the art fracture descriptions (nonlocal microplane model [32], phase-field approach, combined finite-discrete element method [33] etc.) would further validate the abilities of the proposed approach.

Acknowledgment

This research is financially supported by the German Research Foundation (DFG) under grant GRK 2250, project B4. The authors gratefully acknowledge this support. Furthermore, the authors acknowledge the support by the DRESDEN Fellowship Programm.

Please cite this document as: Stochino, F., Qinami, A., Kaliske, M. (2017). Eigenerosion for static and dynamic brittle fracture. Engineering Fracture Mechanics, DOI:10.1016/j.engfracmech.2017.05.025

References

[1] E. Parker, Brittle Behavior of Engineering Structures, National Academy of Sciences, National Research Council, Wiley, New York, 1957.

[2] J. Lund, J. Byrne, Leonardo da vinci's tensile strength tests: implications for the discovery of engineering mechanics, Civil Engineering Systems 18 (2001) 243–250.

[3] A. Griffith, The phenomena of rupture and flow in solids, Philosophical Transaction of the Royal Society A 221 (1921) 163–198.

[4] G. Francfort, J. Marigo, Revisiting brittle fracture as an energy minimization problem, Journal of the Mechanics and Physics of Solids 46 (1998) 1319–1342.

[5] G. D. Maso, R. Toader, A model for the quasi-static growth of brittle fractures: Existence and approximation results, Archive for Rational Mechanics and Analysis 162 (2002) 101–135.

[6] G. Francfort, C. Larsen, Existence and convergence for quasi-static evolution in brittle fracture, Communications on Pure and Applied Mathematics 56 (2003) 1465–1500.

[7] G. D. Maso, G. Francfort, R. Toader, Quasistatic crack growth in nonlinear elasticity, Archive for Rational Mechanics and Analysis 176 (2005) 165–225.

[8] B. Schmidt, F. Fraternali, M. Ortiz, Eigenfracture: an eigendeformation approach to variational fracture, Multiscale Modeling & Simulation 7 (2009) 1237–1266.

[9] T. Mura, Mechanics of Defects in Solids, Martinus Nijhorff, Dordrecht, 1987.

[10] C. Miehe, F. Welschinger, M. Hofacker, Thermodynamically consistent phase-field models of fracture: Variational principles and multi-field fe implementations, Numerical Methods in Engineering 83 (2010) 1273–1311.

Please cite this document as: Stochino, F., Qinami, A., Kaliske, M. (2017). Eigenerosion for static and dynamic brittle fracture. Engineering Fracture Mechanics, DOI:10.1016/j.engfracmech.2017.05.025

[11] Z. Bažant, J. Ožbolt, Nonlocal microplane model for fracture, damage and size effect in structure, Journal of Engineering Mechanics 116 (1990) 2485–2505.

[12] A. Pandolfi, M. Ortiz, An eigenerosion approach to brittle fracture, International Journal for Numerical Methods in Engineering 92 (2012) 694–714.

[13] W. Liu, D. Schesser, Q. Yang, D. Ling, A consistency-check based algorithm for element condensation in augmented finite element methods for fracture analysis, Engineering Fracture Mechanics 139 (2015) 78–97.

[14] E. Ooi, Z. Yang, Modelling crack propagation in reinforced concrete using a hybrid finite element scaled boundary finite element method, Engineering Fracture Mechanics 78 (2011) 252–273.

[15] J. Sancho, J. Planas, D. Cendn, E. Reyes, J. Glvez, An embedded crack model for finite element analysis of concrete fracture, Engineering Fracture Mechanics 74 (2007) 75–86.

[16] M. Kurumatani, K. Terada, J. Kato, T. Kyoya, K. Kashiyama, An isotropic damage model based on fracture mechanics for concrete, Engineering Fracture Mechanics 155 (2016) 49–66.

[17] S. Mitchell, A. Pandolfi, M. Ortiz, Effect of brittle fracture in a metaconcrete slab under shock loading, Journal of Engineering Mechanics 142(4): 04016010.

[18] C. Miehe, M. Hofacker, F. Welschinger, A phase field model for rate-independent crack propagation: Robust algorithmic implementation based on operator splits, Computer Methods in Applied Mechanics and Engineering 199 (2010) 2765–2778.

[19] C. Miehe, Comparison of two algorithms for the computation of fourth-order isotropic tensor functions, Computer & Structures 66 (1998) 37–43.

[20] M. Ortiz, A. Giannakopoulos, Crack propagation in monolithic ceramics under mixed mode loading, International Journal of Fracture 44 (1990) 233–258.

Please cite this document as: Stochino, F., Qinami, A., Kaliske, M. (2017). Eigenerosion for static and dynamic brittle fracture. Engineering Fracture Mechanics, DOI:10.1016/j.engfracmech.2017.05.025

[21] J. Rice, Mathematical Analysis in the Mechanics of Fracture, Academic Press, New York, 1968.

[22] M. Nooru-Mohamed, Mixed-mode fracture of concrete: An experimental approach, Ph.D. thesis, Delft University of Technology (1992).

[23] B. Barr, D. Brokenshire, Torsion fracture tests, BRE Digest, Bracknell, 1996.

[24] D. Brokenshire, A study of torsion fracture test, Ph.D. thesis, Cardiff University (1996).

[25] A. Jefferson, B. Barr, T. Bennet, S. Hee, Three dimensional finite element simulations of fracture tests using the craft concrete model, Computers and Concrete 1 (2004) 261–284.

[26] J. Song, H. Wang, T. Belytschko, A comparative study on finite element methods for dynamic fracture, Computational Mechanics 42 (2008) 239–250.

[27] C. Steinke, C. Özenç, G. Chinaryan, M. Kaliske, A comparative study of the r-adaptive material force approach and the phase-field method in dynamic fracture, Internation Journal of Fracture 201 (2016) 97–118.

[28] H. Schuler, C. Mayrhofer, K. Thoma, Spall experiments for the measurement of the tensile strength and fracture energy of concrete at high strain rates, International Journal of Impact Engineering 32 (2006) 1635–1650.

[29] L. Francesconi, L. Pani, F. Stochino, Punching shear strength of reinforced recycled concrete slabs, Construction and Building Materials 127 (2016) 248–263.

[30] F. Stochino, Rc beams under blast load: Reliability and sensitivity analysis, Engineering Failure Analysis 66 (2016) 544–565.

[31] A. Qinami, I. Zreid, R. Fleischhauer, M. Kaliske, Modeling of impact on concrete plates by use of the microplane approach, International Journal of Non-Linear Mechanics 80 (2016) 107–121.

[32] I. Zreid, M. Kaliske, Regularization of microplane damage models using an implicit gradient enhancement, International Journal of Solids and Structures 51 (2014) 3480–3489.

Please cite this document as: Stochino, F., Qinami, A., Kaliske, M. (2017). Eigenerosion for static and dynamic brittle fracture. Engineering Fracture Mechanics, DOI:10.1016/j.engfracmech.2017.05.025

[33] N. Živaljić, Z. Nikolić, H. Smoljanović, Computational aspects of the combined finite-discrete element method in modelling of plane reinforced concrete structures, Engineering Fracture Mechanics 131 (2014) 669–686.

Please cite this document as: Stochino, F., Qinami, A., Kaliske, M. (2017). Eigenerosion for static and dynamic brittle fracture. Engineering Fracture Mechanics, DOI:10.1016/j.engfracmech.2017.05.025